



Harmful algal blooms and cyanotoxins in Lake Amatitlán, Guatemala, coincided with ancient Maya occupation in the watershed

Matthew Neal Waters^{a,1} , Mark Brenner^{b,c} , Jason Hilleary Curtis^c , Claudia Suseth Romero-Oliva^d, Margaret Dix^d, and Manuel Cano^e

^aDepartment of Crop, Soil and Environmental Sciences, Auburn University, Auburn, AL 36849; ^bLand Use and Environmental Change Institute, University of Florida, Gainesville, FL 32611; ^cDepartment of Geological Sciences, University of Florida, Gainesville, FL 32611; ^dCentro de Estudios Atitlán, Universidad del Valle de Guatemala, Sololá, Guatemala 7001; and ^eAutoridad para el Manejo Sustentable de la Cuenca y del Lago Amatitlán, Villa Nueva, Guatemala 502

Edited by B. L. Turner, Arizona State University, Tempe, AZ, and approved October 15, 2021 (received for review June 1, 2021)

Human-induced deforestation and soil erosion were environmental stressors for the ancient Maya of Mesoamerica. Furthermore, intense, periodic droughts during the Terminal Classic Period, ca. Common Era 830 to 950, have been documented from lake sediment cores and speleothems. Today, lakes worldwide that are surrounded by dense human settlement and intense riparian land use often develop algae/cyanobacteria blooms that can compromise water quality by depleting oxygen and producing toxins. Such environmental impacts have rarely been explored in the context of ancient Maya settlement. We measured nutrients, biomarkers for cyanobacteria, and the cyanotoxin microcystin in a sediment core from Lake Amatitlán, highland Guatemala, which spans the last ~2,100 y. The lake is currently hypereutrophic and characterized by high cyanotoxin concentrations from persistent blooms of the cyanobacterium *Microcystis aeruginosa*. Our paleolimnological data show that harmful cyanobacteria blooms and cyanotoxin production occurred during periods of ancient Maya occupation. Highest prehistoric concentrations of cyanotoxins in the sediment coincided with alterations of the water system in the Maya city of Kaminaljuyú, and changes in nutrient stoichiometry and maximum cyanobacteria abundance were coeval with times of greatest ancient human populations in the watershed. These prehistoric episodes of cyanobacteria proliferation and cyanotoxin production rivaled modern conditions in the lake, with respect to both bloom magnitude and toxicity. This suggests that pre-Columbian Maya occupation of the Lake Amatitlán watershed negatively impacted water potability. Prehistoric cultural eutrophication indicates that human-driven nutrient enrichment of water bodies is not an exclusively modern phenomenon and may well have been a stressor for the ancient Maya.

harmful algal blooms | cyanotoxins | Maya | water quality | ancient

Dense populations of algae and cyanobacteria, called harmful algal blooms (HABs), are global environmental phenomena that are increasing in frequency and magnitude (1, 2). HABs negatively impact ecosystem processes and can lead to water column hypoxia/anoxia, alter aquatic communities, and reduce biodiversity (3, 4). Furthermore, some cyanobacteria release toxins into the environment. Cyanotoxins are metabolites that are capable of affecting the health of humans and other animals through poisoning, oxidative stress, and bioaccumulation (5, 6). Ecological drivers of HABs and cyanotoxin production include climate change [i.e., warmer temperatures (4, 7)] and cultural eutrophication [i.e., excessive urban or agricultural nutrient inputs (1, 2, 8)]. Prevention and mitigation of HABs and cyanotoxin production are of tremendous concern and are receiving considerable attention (9–11). Few studies, however, have investigated whether ancient human populations caused or were affected by toxic algal blooms (12, 13). One ancient society, known to have achieved high population

densities and caused profound land cover changes, was the Maya of Mesoamerica.

Maya culture first arose >3,000 y ago and experienced a florescence during the Classic Period, from ca. Common Era (CE) 250 to 900 (14). Classic Maya cities of the Mesoamerican lowlands were densely populated, and urban centers relied on intensive agricultural practices, which were associated with environmental impacts such as deforestation (15) and soil erosion (16–18). In the past few decades, evidence of profound climate changes during the period of Maya occupation has emerged, and ancient droughts in the Maya region were shown to have been temporally correlated with times of sociopolitical disintegration (19–24). Whereas these multiple environmental stressors probably affected ancient Maya society, individually and/or in concert, far less attention has been directed at exploring ancient, human-mediated changes in water quality. A few studies, however, have shown the importance of water characteristics to the ancient Maya (25) and documented water quality changes in Yucatán and Belize during the Classic Period (26, 27). A recent study that conducted 16S ribosomal rRNA amplicon sequencing on sediments from reservoirs at the

Significance

Harmful algal blooms (HABs) are dense populations of algae and/or cyanobacteria that can harm aquatic ecosystems by reducing water column oxygen and producing toxins. Whereas HABs are well documented in modern lakes, there has been little research on HABs associated with ancient societies. We inferred the magnitude of past HABs using a sediment core from Lake Amatitlán, Guatemala, which hosted large, prehistoric Maya populations in its watershed and currently experiences toxic HABs. About 1,000 y ago, ancient Maya in the area experienced periods of intense HABs and cyanotoxin concentrations in the lake, which rivaled the degraded conditions in the water body today. Human-associated HABs have affected both modern and ancient societies and deserve attention when exploring past human–environment interactions.

Author contributions: M.N.W., M.B., J.H.C., and M.D. designed research; M.N.W., M.B., J.H.C., C.S.R.-O., and M.C. performed research; M.N.W. contributed new reagents/analytic tools; M.N.W., M.B., J.H.C., C.S.R.-O., and M.D. analyzed data; and M.N.W., M.B., J.H.C., C.S.R.-O., M.D., and M.C. wrote the paper.

The authors declare no competing interest.

This article is a PNAS Direct Submission.

This open access article is distributed under [Creative Commons Attribution-NonCommercial-NoDerivatives License 4.0 \(CC BY-NC-ND\)](https://creativecommons.org/licenses/by-nc-nd/4.0/).

¹To whom correspondence may be addressed. Email: mwaters@auburn.edu.

This article contains supporting information online at <http://www.pnas.org/lookup/suppl/doi:10.1073/pnas.2109919118/-DCSupplemental>.

Published November 22, 2021.

ancient Maya city of Tikal (Guatemala) showed that two cyanobacteria genera capable of producing toxins, *Planktothrix* and *Microcystis*, were present at the site (28). Cyanotoxin measurements, however, were not undertaken. Concentrations of photosynthetic pigments (29, 30) and cyanotoxins (31, 32) can, however, be measured in lake sediments, making it possible to infer the magnitude of past HABs and their toxin production through time.

The Lake Amatitlán watershed in highland Guatemala (Fig. 1) hosted the pre-Columbian Maya city of Kaminaljuyú, a major urban center during the Preclassic and Classic Periods, with ancient population numbers that rivaled urban centers in the Maya Lowlands (33). Whereas highland Maya areas have received less attention than lowland sites, with respect to past human demography, environmental degradation, and the Terminal Classic “collapse,” the Valley of Guatemala was home to dense Maya populations and subject to land use intensification, extensive agriculture, and changes in water quantity, similar to the lowlands (34–36). Today, Lake Amatitlán is hypereutrophic, with persistent, dense HABs, low water clarity (Secchi depths 0.1 to 0.8 m) (37), and high concentrations of the cyanotoxin microcystin, with mean values of $90 \mu\text{g} \cdot \text{L}^{-1}$ (extracellular) and $1,931 \mu\text{g} \cdot \text{L}^{-1}$ (intracellular) (38), the latter prone to settling out of the water column and accumulating in the lake sediments. The World Health Organization provisional guideline value for microcystin-LR concentration in inland waters is $1 \mu\text{g} \cdot \text{L}^{-1}$ (39). Lake Amatitlán hydrology is largely dominated by inputs from the Villalobos River, which drains a substantial portion of the Valley of Guatemala watershed (Fig. 1). Water is also delivered to the lake by direct rainfall, overland drilling, and discharge from small streams, but these hydrologic inputs are small compared with inflow from the Villalobos River.

We conducted a paleolimnological study, using a sediment core from Lake Amatitlán, to address two research questions: 1) did Lake Amatitlán experience HABs and cyanotoxin production during the period of ancient Maya occupation? and 2) if so, how closely did water quality degradation track documented human occupation in the catchment? We collected a

550-cm sediment core in 2019 from a site in the lake where cores for previous paleolimnological studies have been obtained (36, 40). Core chronology was established using 10 accelerator mass spectrometry radiocarbon (AMS ^{14}C) dates and Bayesian statistics, which showed that we had retrieved a $\sim 2,100$ -y record of continuous sediment accumulation that extends from the Maya Late Preclassic Period to present. We measured concentrations of nutrients (organic carbon, total nitrogen, total phosphorus, and total sulfur), photosynthetic pigments, and cyanotoxins (total microcystins) in samples throughout the core.

Results

The 550-cm-long core from Lake Amatitlán represents continuous sediment accumulation from ca. 110 BCE to the collection date in CE 2019. The Bayesian age-depth model combined five AMS ^{14}C samples from the core reported here with five samples from a core collected at a nearby location in 2012 (40) (Table 1). Dates from the previously published core were projected onto the 2019 core by first aligning depths in the cores that yielded identical dates and then matching magnetic susceptibility peaks in the two profiles (*SI Appendix, Fig. S1*). The Bayesian model, calculated using the BACON package in R (41), assigned a date of $\sim 110 \text{ BCE} \pm 110$ to the base of the core and a date of $\text{CE } 2015 \pm 5$ to the core top, thus spanning from the Maya Late Preclassic to present (*SI Appendix, Fig. S2*).

The sediment core was divided into four stratigraphic zones, using *k*-means cluster analysis on principal components 1 and 2 for all measured data, with the exception of the cyanobacteria pigment echinenone (Fig. 2, *SI Appendix, Fig. S3*, and Table 2). Zone I extends from the base of the core to CE 550 and represents a period of relatively lower trophic status (i.e., moderate nutrient concentrations). Carbon, nitrogen, and sulfur concentrations are low compared with values in other core zones, but phosphorus concentrations display intermediate levels (Table 2). Total primary producer abundance, represented by the concentration of the photosynthetic pigment beta carotene, was lower than in any other zone ($40.3 \pm 17.9 \text{ nmol} \cdot \text{g}^{-1} \text{ org}$

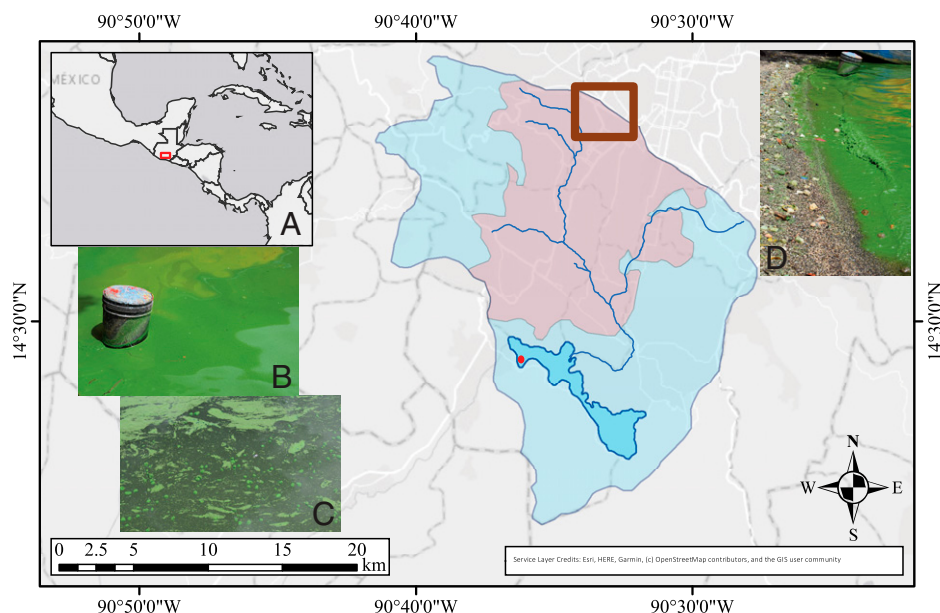


Fig. 1. Map of the Valley of Guatemala, showing the location of Lake Amatitlán. The blue area is the lake watershed, and the pink area is the modern metropolitan area of Guatemala City. The brown box shows the location of the ancient Maya site of Kaminaljuyú, and the red dot in the lake indicates the sediment coring site. *Insert A* shows the location of the Guatemala highlands in Central America. *Inserts B, C, and D* show cyanobacteria blooms in the lake. Photographs used with permission from the National Geographic Society.

Table 1. Radiocarbon dates from the Lake Amatitlán core, used to construct the depth-age model with the BACON R package

Sample no.	Depth in centimeters (ref. 40, depth)	Age 14C y BP*	Cal date (BCE/CE, 2 sigma)†
Core top	0	-69	CE 2019
WH-168107	109	120 ± 15	CE 1808 to 1924
PLD-28983	309 (243)	845 ± 15	CE 1161 to 1247
WH-168108	330	790 ± 40	CE 1201 to 1283
PLD-28985	405 (289)	1,270 ± 20	CE 682 to 771
WH-168109	405	1,270 ± 20	CE 670 to 775
PLD-28986	411 (312)	1,445 ± 20	CE 581 to 648
PLD-28987	420 (323)	1,495 ± 20	CE 541 to 613
PLD-28988	441 (364)	1,605 ± 20	CE 403 to 536
WH-168110	503	1,830 ± 20	CE 153 to 250
UGA-45272	540	2,150 ± 35	231 to 88 BCE

PLD samples are from Lohse et al. (40), and depth equivalents in our core were assigned by matching magnetic susceptibility profiles (*SI Appendix, Fig. S1*). Depths in the Lohse et al. (40) core are in parentheses. Abbreviations: BP, before present; Cal, calibration; PLD-XXXXX, ¹⁴C laboratory number for ref. 40 samples.

*Ages are in radiocarbon years before present.

†Ages calibrated using CALIB 8.2 (60).

[organic matter]), suggesting relatively higher water clarity during this period. Primary producer community structure was dominated by diatoms, as indicated by abundance of the pigment diatoxanthin, with lower concentrations of cyanobacteria, recorded by the pigments canthaxanthin and echinenone. A third cyanobacteria pigment, aphanizophyll, present in more recent core zones, was absent during Zone I (Table 2). Cyanotoxin concentrations were at moderate levels during Zone I, with a spike of 84 ng · g⁻¹ org at CE 290.

Sediment core Zone II spanned from CE 550 to 1200 and represents a period of increased lake trophic state, with high nutrient concentrations and dominance of cyanobacteria. Pigment data indicate that cyanobacteria replaced diatoms as the dominant primary producers, with the highest average concentrations for the cyanobacteria pigment canthaxanthin (52.9 ± 28.1 nmol · g⁻¹ org) and the total abundance indicator beta carotene (220 ± 139.3 nmol · g⁻¹ org), relative to other prehistoric Zones (I and III) (Table 2). Concentrations of echinenone, a pigment that is often found in extremely high concentrations in *Microcystis* spp (42), were greatest during Zone II, with an average of 93.9 ± 79.6 nmol · g⁻¹ org, an order of magnitude higher than in the other zones that contain prehistoric deposits (Zones I and III). Average nutrient concentrations of organic carbon and sulfur were highest in this zone and comparable to values

in modern-day sediments, with averages of 4.88 ± 1.5% and 9.92 ± 4.0 mg · g⁻¹, respectively. Molar ratios of nutrients C/N and N/P were both higher during Zone II than in any other period, indicating that this time was characterized by a unique combination of nutrient inputs and biogeochemical conditions. Beta carotene concentrations displayed peaks of 746 and 520 nmol · g⁻¹ org at CE 850 and 1050, respectively, similar to concentration peaks of 487 and 902 nmol · g⁻¹ org in the two top-most, modern sediment samples. Despite high cyanobacteria pigment concentrations, cyanotoxin concentrations remained at relatively low levels during most of Zone II, except for a spike of 65 ng · g⁻¹ org ca. CE 1050, which coincided with spikes in beta carotene and cyanobacteria pigments.

Core Zone III spanned from CE 1200 to 1942, which included European colonization that began in the mid-1500s. Nitrogen, carbon, and sulfur concentrations in Zone III returned to lower values, similar to those in Zone I, and a decline in the concentrations of photosynthetic pigments indicates a decrease in lake trophic state. Phosphorus, however, increased during this zone, beginning around CE 1600. Primary producer community structure included a return to diatom dominance, with a mean diatoxanthin concentration of 66 ± 49.2 nmol · g⁻¹ org, around twice the average values in Zones I and II (Table 2). Cyanotoxin concentration increased to

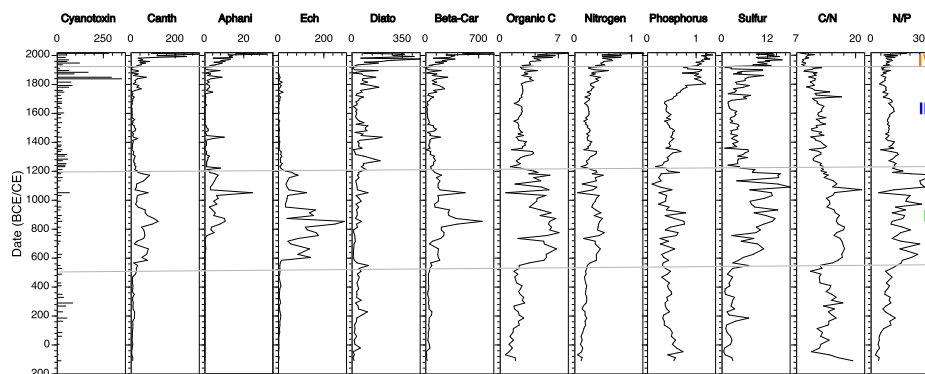


Fig. 2. Date (BCE/CE) versus paleolimnological variables in the Lake Amatitlán sediment core. Ages were assigned using Bayesian statistics and the Bacon package in R (41). Cyanotoxin is total microcystins reported as ng toxin · g org⁻¹. Pigments Canth (canthaxanthin), Aphani (aphanizophyll), Ech (echinenone), Diato (diatoxanthin), and Beta-Car (beta carotene) are reported as nmol pigment · g org⁻¹. Canthaxanthin, aphanizophyll, and echinenone are biomarkers for cyanobacteria (29). Echinenone values presented only for sediments older than ca. CE 1940. Diatoxanthin is a biomarker for diatoms, and beta carotene is a proxy for total primary producer abundance. Organic carbon and nitrogen are reported as percent of dry sediment mass, phosphorus and sulfur are reported as mg · g⁻¹ dry sediment. C/N and N/P are molar ratios calculated from mass concentrations. Sediment core Zones (I, II, III, and IV) were determined by *k*-means cluster analysis on principal components 1 and 2 (*SI Appendix, Fig. S3*).

Table 2. Average concentrations and SDs, in parentheses, for each variable in the four sediment zones

Variable	Unit	Zone I	Zone II	Zone III	Zone IV
Total microcystin	ng g ⁻¹ org	28.74 (18)	21.3 (11)	51.1 (70.5)	101.1 (91)
Phosphorus	mg g ⁻¹	0.44 (0.1)	0.41 (0.2)	0.60 (0.3)	1.17 (0.1)
Nitrogen	%	0.17 (0.04)	0.36 (0.1)	0.28 (0.1)	0.63 (0.2)
Organic carbon	%	1.96 (0.6)	4.88 (1.5)	2.67 (0.7)	4.81 (1.4)
Sulfur	mg · g ⁻¹	2.29 (1.6)	9.92 (4.0)	4.39 (2.5)	12.0 (2.3)
C/N		13.74 (2.0)	15.67 (1.7)	11.49 (1.4)	8.95 (0.8)
N/P		8.97 (3.5)	21.52 (7.9)	11.02 (2.9)	12.01 (3.8)
Aphanizophyll*	nmol · g ⁻¹ org	0	4.4 (4.7)	1.6 (2.1)	12.2 (6.6)
Diatoxanthin	nmol · g ⁻¹ org	38.7 (25.7)	33.1 (20.6)	66.0 (49.2)	245 (133)
Canthaxanthin*	nmol · g ⁻¹ org	9.7 (6.7)	52.9 (28.1)	13.7 (12.7)	105 (88)
Beta carotene	nmol · g ⁻¹ org	40.3 (17.9)	220.0 (139.3)	77.9 (59.6)	323 (197)
Total cyanobacteria [†]	nmol · g ⁻¹ org	9.7 (6.7)	57.4 (30.3)	15.2 (14.1)	117 (93)
Echinenone	nmol · g ⁻¹ org	4.9 (2.9)	93.9 (79.6)	6.4 (6.3)	

*Cyanobacteria pigments.

[†]Total cyanobacteria is the sum of aphanizophyll and canthaxanthin.

moderate levels, with spikes around 50 ng · g⁻¹ org at ca. CE 1250, 1280, and 1320 but decreased to relatively low levels around CE 1350. The highest concentration of microcystin occurred around CE 1820, with values > 250 ng · g⁻¹ org.

Sediment core Zone IV was deposited in the last ~80 y and documents the development of the hypereutrophic and toxin-rich conditions that characterize the lake today. All nutrient concentrations increased from the base of the zone to present, with the highest average concentrations for N (0.63 ± 0.2%) and P (1.17 ± 0.1 mg · g⁻¹) in this zone. Average photosynthetic pigment concentrations in Zone IV were highest for all pigments measured except echinenone, which could not be

quantified in this zone (Table 2). Whereas *Microcystis* spp. dominate in Lake Amatitlán today (38) and would be represented in the sediment record by the pigment echinenone, other cyanobacteria taxa such as *Oscillatoria* spp. and *Aphanizomenon* spp. are also abundant (43) and likely account for the high non-echinenone cyanobacteria pigments in Zone IV. Cyanotoxin levels were high throughout Zone IV, with an average concentration of 101.1 ± 91 ng · g⁻¹ org. The maximum concentration of 278 ng · g⁻¹ org occurred around CE 2015.

Multivariate statistics (PCA) show that Zones I and III were similar with respect to measured sediment components and that Zone II and most recent Zone IV were similar

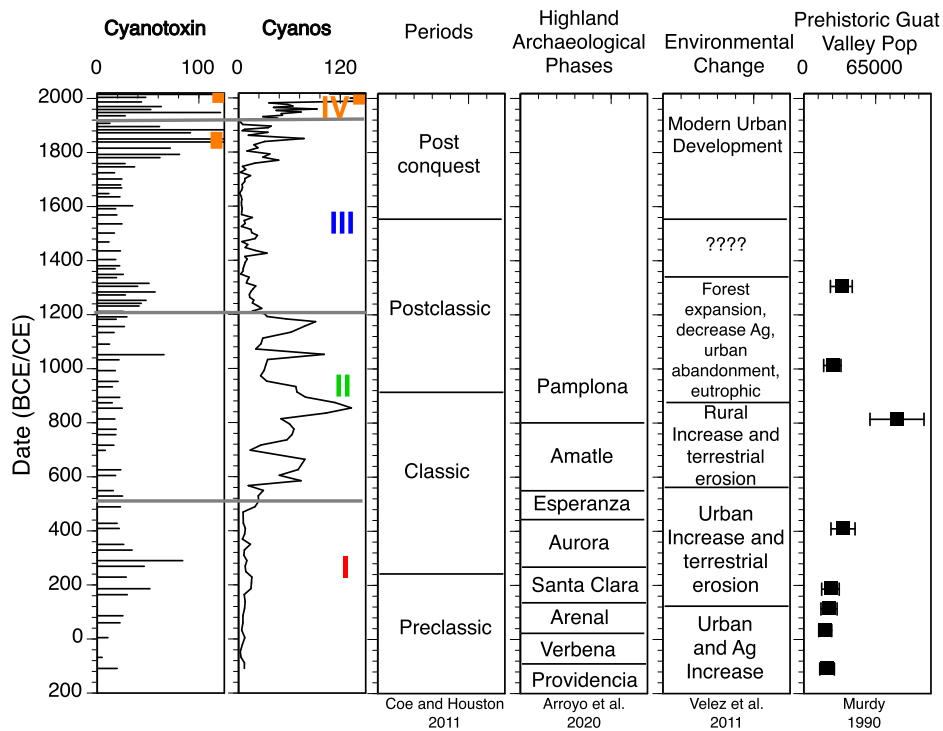


Fig. 3. Date (BCE/CE) versus paleolimnological variables for Zones I, II, III, and IV in the Lake Amatitlán sediment core. Cyanobacteria pigments (Cyanos) are the sum of concentrations of aphanizophyll and canthaxanthin. Cyanotoxin data are shown on abbreviated axis scales to better illustrate stratigraphic changes that occurred during zones spanning Maya prehistory. Times when concentrations exceeded the maximum scale values are indicated by orange squares. Maya prehistory periods are those described in Coe and Houston (14). Highland archaeological phases are based on pottery sequences and a Bayesian dating model (35). Paleoenvironmental changes were inferred from diatom, pollen, and geochemical variables (36) in a core collected from the a nearby site as the core reported here. Estimated ancient population numbers in rural areas of the Lake Amatitlán watershed (44), with dates modified using the updated dating model from Arroyo et al. (35).

(*SI Appendix, Fig. S3*). Principal components 1 (PC1) and 2 (PC2) explained 50 and 21% of the data, respectively. PC1 separated Zones I and III from Zones II and IV and indicated higher nutrient concentrations and more eutrophic conditions in the latter two zones. PC2 showed a separation in the ordination of Zones II and IV, with eigenvectors of organic carbon, N/P, canthaxanthin, and beta carotene ordinating more with Zone II, and eigenvectors of microcystins, diatoxanthin, and phosphorus (P) ordinating with Zone IV (*SI Appendix, Table S1*). Whereas both Zones II and IV are inferred to have been times of substantial HABs, the different eigenvectors associated with each zone indicate that the drivers of eutrophication were linked with multiple elements associated with terrestrial and riverine inputs for Zone II and P inputs for Zone IV. The separation also highlights the high cyanotoxin concentrations in Zone IV, which were lacking in Zone II.

Discussion

The paleolimnologically inferred trophic state history of Lake Amatitlán extends from the Late Preclassic Period (ca. 110 BCE) to present and shows that the lake experienced eutrophic conditions and cyanotoxin production during pre-Columbian Maya occupation of the Valley of Guatemala. Whereas the modern hypereutrophic condition of the lake is characterized by both high cyanobacteria biomass and cyanotoxin production, prehistoric dense cyanobacteria abundance did not coincide with the periods of highest cyanotoxin concentration. Despite asynchrony of these two sediment indicators of past eutrophy, comparisons with concentration values in recent Amatitlán sediments show that the ancient highland Maya experienced HABs that were similar in intensity to those in the modern lake and that ancient watershed inhabitants likely had to contend with compromised water quality (Fig. 3), as did the ancient Maya at some lowland sites during the Classic Period (25, 27).

Prehistoric Eutrophication and HABs. The base of the core dates to ~110 BCE, during which time the lake hosted lower cyanobacteria abundance than at other times in the record. The earliest period includes the Late Preclassic to Early Classic transition and corresponds to the highland ceramic phases of Providencia, Verbena, Arenal, and Santa Clara (Figs. 2 and 3). Moderate nutrient input from the landscape occurred, as suggested by relatively high C/N values and magnetic susceptibility (Fig. 2 and *SI Appendix, Fig. S1*). This period lasted until about CE 550 and coincided with shifting population numbers at Kaminaljuyú (34, 35), which included increases in rural populations in the Valley of Guatemala [Fig. 2 (44)]. Relatively low values of cyanobacteria pigments canthaxanthin and aphanizopyll during this period appear at odds with the cyanotoxin values, suggesting that cyanobacteria taxa that were not recorded in the pigment record may nevertheless have existed at that time. This, however, is unlikely, given that concentrations of echinenone, a dominant pigment in *Microcystis* spp (42), were also low (Fig. 2 and Table 2). In addition, the high cyanotoxin values coincided with relatively high diatom abundance, as indicated by diatoxanthin concentrations (Fig. 2). Shifts in the occurrence of diatoms and cyanotoxin production, together with archaeologically derived demographic data, suggest that limnological changes corresponded with alterations of urban centers in the watershed.

Zone I also corresponds to an interval of higher concentrations of *Zea* pollen, derived from local agriculture (36), and to the time of drying of Lake Miraflores at the urban site of Kaminaljuyú (34, 36), which could have altered nutrient inputs and the form of organic matter that entered Lake Amatitlán. In addition, hydrological changes could have occurred in the watershed, as canals that had been used to move water from

Lake Miraflores to other areas in the Valley of Guatemala fell out of use around the same time (36). Although it has not been confirmed that the change in water management was drought-related, a shift in agricultural practices is believed to have occurred and may well have caused the subsequent nutrient regime changes and accounted for the cyanotoxin occurrence.

Sediment core Zone II extends from ca. CE 550 to 1200, a time when Lake Amatitlán experienced an increase in cyanobacteria abundance, as shown by higher concentrations of pigments canthaxanthin, aphanizopyll, and echinenone (Fig. 2), which are diagnostic for cyanobacteria (29). With the exception of echinenone, however, these pigments are low in microcystin-producing species, which could explain the low microcystin concentration during this period. This zone spans the Late Classic to early Postclassic Periods and includes the Terminal Classic “collapse,” documented at many Lowland Maya archaeological sites (14). Studies of sediment cores from Lake Chichancanab (19, 20) and cave speleothems from elsewhere on the low-elevation Yucatán Peninsula (21) provided evidence of a series of extreme droughts during this period. Highland areas, and specifically the Valley of Guatemala, however, are not known to have experienced droughts at that time. Pollen data show increases in taxa such as *Quercus* and *Pinus* during this period, which suggest it was a time of forest recovery (36). Agricultural practices changed during this period, and there was a decline in the urban population of Kaminaljuyú, in the northern part of the watershed (34), while the rural population increased (44). Volcanic soils in the region are fertile, suggesting they are capable of producing continuous high crop yields despite extensive land alteration (45). Watershed inputs are evident from increases in C/N and nutrient concentrations, which suggest substantial input of material from the Lake Amatitlán watershed via the Villalobos River, in agreement with previous paleolimnological inferences (36).

High concentrations of all cyanobacteria pigments and the total abundance pigment beta carotene in sediment core Zone II indicate that recent, ongoing cultural eutrophication in Lake Amatitlán (Zone IV) is not unique in the lake’s trophic state history (Fig. 2 and Table 2). Because photosynthetic pigments degrade through time, it is likely that pigment concentrations in sediments of Zone II, at the time of deposition, were greater than what we measured (46). We conclude that HABs during the Late Classic and early Postclassic Periods were of a magnitude similar to the extreme HABs in the lake today. The period of high cyanobacteria pigment abundance corresponds to lower diatom pigment concentration and higher C, N, P, and N/P (Figs. 2 and 3). Nutrient influx was likely associated with material inputs from the surrounding landscape and delivered by the Villalobos River and triggered HABs in the lake.

Sediment core Zone III followed the prehistoric eutrophic period and was characterized by a decrease in cyanobacteria abundance, a decrease in overall phytoplankton abundance, an increase in diatom abundance, and declines in organic carbon and N/P in the sediment. This period, which extended from CE 1200 until the 1900s, coincided with declining Maya population in the Valley of Guatemala (44) and decreases in terrestrial inputs, as revealed by lower C/N and nutrient (N and P) concentrations (Fig. 2) linking these nutrient inputs with the period of European conquest in the area (14). Phosphorus, however, began to increase around CE 1600 and continued to increase throughout the zone. Grains of *Quercus* and *Pinus* still dominated the pollen spectra, indicating forest vegetation was widespread in the watershed (36). HABs were not as intense as those recorded in Zone II, as revealed by lower cyanobacteria pigment concentrations, but cyanotoxin abundance was relatively high compared with Zones I and II. Likewise, Zone III experienced the only prehistoric increase in the ratio of chlorophyll to pheophytin concentrations, which suggests improved

conditions for pigment preservation and supports the notion that low pigment concentrations in the zone are indicative of improved water quality (*SI Appendix, Fig. S4*).

Sediment core Zone IV encompasses the period of recent HABs that continue to affect Lake Amatitlán today. High cyanobacteria abundance and microcystin values in the modern lake are attributed to excessive nutrient inputs that originate from the metropolitan area of Guatemala City and are delivered by the Villalobos River. Whereas sediments from earlier eutrophic periods in Lake Amatitlán's history also contained high concentrations of cyanobacteria pigments and nutrients (Zone II), Zone IV sediments stand out in the Lake Amatitlán paleolimnological record in also having very high cyanotoxin concentrations. Occurrence of high cyanotoxin values in near-surface deposits (Fig. 3) is not surprising, as recent limnological studies have documented intense HABs in Lake Amatitlán (37, 38).

Paleolimnology of Cyanotoxins in Lake Amatitlán. Analysis of cyanotoxins in lake sediments is still being developed as a paleolimnological tool, but several studies have applied such measurements successfully to sediment records that span the last ~150 y (31, 47), and another study interpreted the cyanotoxin record over the last ~4,700 y (32). Microcystins are water soluble and are delivered to lake sediment as intracellular components of cyanobacteria cells (5, 6, 8, 47), and studies of postdepositional cyanotoxin transformations are ongoing (47). Asynchronicity between cyanobacteria pigment abundance and cyanotoxin concentration in Zones I, II, and III of the Lake Amatitlán core could have resulted from several factors: 1) shifts in cyanobacteria community structure, 2) changes in environmental conditions that trigger microcystin production, 3) alteration of conditions that govern rates of degradation of pigments and cyanotoxins, and 4) postdepositional mobility of water-soluble toxins, in contrast to the fixed stratigraphic position of water-insoluble pigments. Nevertheless, concentrations of total microcystins throughout the Lake Amatitlán core provide evidence that cyanotoxins were present in the water column during the period of ancient Maya settlement in the Valley of Guatemala.

During Zone I, cyanotoxin concentrations were as high or higher than at any other time, with the exception of Zone IV (i.e., the last ~80 y). Cyanotoxin concentration in sediment Zone I increased between CE 180 and 400 (Fig. 2). Whereas greater cyanobacteria abundance does not necessarily trigger more cyanotoxin production (6), shifts in the element stoichiometry in the sediments, such as the decrease in N/P and increase in C/N, suggest a change in biogeochemical processes and increases in organic matter recalcitrance during that time interval. In Zone II, association of relatively high cyanobacteria pigments and low cyanotoxins was not entirely unexpected and is consistent with what has been seen in some lakes undergoing recent cultural eutrophication. In contrast to modern, microcystin-rich HABs in Lake Amatitlán, however, cyanotoxin concentrations in Zone II remained relatively low. One peak in microcystin concentration, however, occurred ca. CE 1050 and corresponds to spikes in cyanobacteria pigments echinenone and aphanizopyll and declines in organic C and N/P (Fig. 2). This isolated event also corresponds to a volcanic tephra deposit (40), which may have supplied the necessary elements to initiate cyanotoxin production in the lake. Although the ecological factors that cause cyanotoxin production are still debated (6), rapid changes in nutrient inputs and stoichiometric ratios have been proposed as triggers (6, 8, 48). Zone III had a similar ordination with Zone I in the PCA. The period of high cyanotoxin concentration in Zone III corresponded to lower N/P, again suggesting that a shift in lake water chemistry was associated with toxin production (*SI Appendix, Fig. S3*). Cyanotoxin

concentrations decreased to low levels about CE 1380 and maintained such concentrations until ca. CE 1800, when the modern hypereutrophic period began.

Water Quality and the Prehistoric Maya. The pigment and cyanotoxin data from Lake Amatitlán contribute to the growing evidence that suggests that the prehistoric Maya faced declines in water quality (25–28, 49). Paleolimnological investigations in the Maya Lowlands found evidence for declines in water quality [e.g., in the reservoirs that served the major center of Tikal in Guatemala (28) the Three Rivers Region of Belize (25), and a smaller settlement near Lake Sayauil, Mexico (49)]. Lentz et al. (28) identified genetic markers for two cyanobacteria genera and inferred that a consequent decrease in water quality, in concert with drought conditions during the Terminal Classic, negatively impacted Maya inhabitants of Tikal. Whereas there is no evidence that drought conditions affected the highland Maya during the Late or Terminal Classic, eutrophic conditions in Lake Amatitlán at that time may have been a stressor for the ancient residents of the Valley of Guatemala. Luzzadder-Beach and Beach (25) showed that changes in water chemistry limited agricultural and domestic water use in prehistoric Maya contexts. Changes in trophic state of lowland Lake Sayauil were inferred from diatoms in a sediment core and coincided with initial settlement during the Preclassic Period (49). Elsewhere in the Maya Lowlands, ancient eutrophication of Lake Cobá was linked to human land alterations and soil erosion (49), as has been the case for recent changes in the nutrient status of many water bodies worldwide (50, 51). Recent eutrophication in Lake Petén-Itzá has been documented (52), but massive siltation in ancient times probably prevented the biological consequences of nutrient enrichment (53). Whereas cyanobacteria abundance in Lake Amatitlán occurred during periods of increased nutrient input, cyanotoxin production coincided with shifts in nutrient stoichiometry (N/P) and, perhaps, as yet unidentified drivers.

HABs in the reservoirs at Tikal and diatom-inferred eutrophication in Lake Sayauil likely impacted the potability of water for people who lived near those sites. Use of Lake Amatitlán by the ancient occupants of the Valley of Guatemala is not well-studied. Lake Amatitlán lies at the south end of the watershed, whereas the Maya city of Kaminaljuyú was located farther north in the watershed, 16 km north of the lake. There is evidence that smaller hamlets were established throughout the Valley during periods when the population of Kaminaljuyú declined (54, 55), times that coincided with the prehistoric eutrophic period (Zone II, Fig. 3). Furthermore, archaeological investigations along the shore of Lake Amatitlán uncovered sites that were occupied beginning in the Preclassic. The largest settlement consisted of several mounds and a ballcourt constructed during the Classic Period, which suggests permanent settlement, rather than construction solely for ceremonial purposes (56). This larger settlement coincided with the early eutrophic period in Lake Amatitlán, as inferred from our core, and indicates the Maya influenced the lake during the prehistoric HAB episode. Furthermore, early accounts of Spanish conquistadors indicate that areas around Lake Amatitlán were densely settled during the mid-16th century (57).

The paleolimnological record from Lake Amatitlán provides evidence of HABs and cyanotoxin production during the period of ancient Maya occupation in the Valley of Guatemala. Whereas climate fluctuations, deforestation, and soil erosion were shown to have been environmental stressors for prehistoric Maya populations, the sediment record from highland Lake Amatitlán, deposits in lowland reservoirs at Tikal (28), and decreases in water quality in the Yucatán Peninsula (27) and Three Rivers region of Belize (25) provide evidence that human-mediated degradation of water quality may have been

an additional, and, perhaps widespread, stressor for the ancient Maya. Development of techniques that enable inference of past HABs and cyanotoxin production from sediment cores (30, 31) opened opportunities to further investigate whether degraded water quality can be added to the list of established societal stressors for the Classic Maya and other ancient societies.

Materials and Methods

Study Site and Core Collection. Lake Amatitlán lies in a volcanic basin in the highlands of Guatemala, south of Guatemala City. The lake is at ~1,186 m above sea level, has a surface area of 15.2 km² and a maximum depth of ~33 m. It receives hydrologic input from precipitation (1,166 mm · yr⁻¹) and from the Villalobos River, which drains the 313 km² watershed of metropolitan Guatemala City (36, 37). The recent hypereutrophic state of the lake was first documented in the 1950s by Deevey (58), when total phosphorus concentration in surface waters was 60 µg · L⁻¹ but which increased to 440 µg · L⁻¹ by the 1980s (36). Secchi disk ranges from 0.1 to 0.8 m, and pH is ~9.3 (37).

A 550-cm-long sediment core was collected in the northwest end of the lake at a water depth of ~12 m, about 160 m from the shoreline. The core site is near the location where sediment cores that yielded radiocarbon-dated records had been collected earlier (36, 40). The 76-cm-long mud–water interface core section was obtained using a piston corer designed to collect undisturbed samples of unconsolidated uppermost sediments (59). Beginning at 50 cm, a modified Livingstone corer was used to collect five subsequent 1-m sections. The mud–water interface core was extruded vertically in the field, sectioned at 4-cm intervals, and stored in labeled Whirl-pak bags. The deeper, consolidated 1-m sediment sections were kept in their labeled polycarbonate core barrels, and all sediments were transported to the Land Use and Environmental Change Institute at the University of Florida. The lower intact sections were measured for gamma ray density and magnetic susceptibility on a Geo-Tek Multi-Sensor core logger (MSCL), after which they were cut lengthwise and digitally imaged using the MSCL, which had also been used for analysis of cores taken previously from Lake Amatitlán. Split core sections (50 to 550 cm) were sampled at 5-cm intervals and, along with the mud–water interface core samples, subjected to paleolimnological analyses.

AMS ¹⁴C Dating and the Age-Depth Model. Five charcoal samples were collected throughout the core for AMS ¹⁴C dating (Table 1). Sediment was sieved through 1-mm mesh to remove fine particles and retained material was examined under a dissecting microscope at 40× to collect charcoal fragments. The deepest sample (540 cm) was analyzed at the Center for Applied Isotope Studies at the University of Georgia (<https://cais.uga.edu/>), and the remaining four samples were sent to the National Ocean Sciences Accelerator Mass Spectrometry Laboratory at the Woods Hole Oceanographic Institute (<https://www.whoi.edu/site/nosams/>). AMS ¹⁴C dates were calibrated using the CALIB 8.20 program (60). Five additional dates, from a sediment core taken earlier at a nearby location (40), were projected onto depths in our core. That was achieved using identical radiocarbon dates for depths in the two cores, 1,270 ± 20 at 405 cm in our core and 289 cm in the Lohse et al. (40) core and then matching magnetic susceptibility peaks in the two profiles (*SI Appendix, Fig. S1*). The 10 dates came from depths that ranged from 109 to 540 cm and were used in the Bayesian dating model BACON in R studio (41).

Elemental, Photosynthetic Pigment, and Cyanotoxin Analysis. Organic matter was measured by weight loss on ignition at 550 °C in a muffle furnace for 2 h. Organic C and N were measured using a Costech Carbon-Hydrogen-Nitrogen Elemental Analyzer, following pretreatment with HCl fumigation in a desiccator to remove carbonates (61). Phosphorus and sulfur were measured on an ARL 3560AES inductively coupled plasma following 15N HNO₃ digestion for 90 min in a heated block (62).

Chlorophylls and carotenoids were measured using a high-performance liquid chromatography (HPLC) system following the methods of Leavitt and Hodgson (29) and Waters et al. (30). Photosynthetic pigments were measured within 90 d of collection and include all pigments used in this study (alloxanthin, aphanizophyll, beta carotene, canthaxanthin, chlorophyll a, diatoxanthin, echinenone, fucoxanthin, lutein+zeaxanthin, and pheophytin a). Primary producer groups associated with each pigment can be found in Leavitt and Hodgson (29). Briefly, dried sediment samples were extracted with a solvent mixture of acetone, methanol, and water (80:15:5 by volume), which contains an internal standard (Sudan II; Sigma Chemical Corp.). Extraction was done for 16 to 24 h in a -20 °C freezer. Samples were injected into a Shimadzu HPLC system following the mobile phase and time sequence of Leavitt and Hodgson (29). Chlorophylls and carotenoids were separated by passing through a

Phenomenex Luna C18 column and measured using a photodiode array detector coupled with a fluorescence detector. Pigments were identified using retention times and pigment-specific spectra of known standards (DHI Lab Products). Pigment concentrations are expressed as nmol pigment · g⁻¹ organic matter (loss on ignition) and were calculated by comparing peak areas against standards of known concentration. The cyanobacteria pigment echinenone was not analyzed in uppermost sediments (Zone IV) of the core because of interference from an unidentified chlorophyll-like pigment peak that overlapped with the echinenone peak. We therefore report echinenone concentrations only for core Zones I, II, and III.

Cyanotoxins as total microcystins were measured on samples throughout the core using the total microcystin/nodularin ADDA enzyme-linked immunoassay (ELISA) kit by Eurofins, purchased from Fisher Scientific (<https://www.fishersci.com/us/en/home.html>). This method was chosen because of its ability to identify all 84 microcystin congeners that can exist in aquatic environments. Presence of microcystins was verified by HPLC, following the methods of Purdie et al. (63). Total microcystins were extracted from dried sediment samples following the combined extraction methods of Zastepa et al. (31) and Eurofins (<https://abraxis.eurofins-technologies.com/home/>). Briefly, sediment samples were extracted with a solvent mixture of 75% methanol and 25% water, along with 0.05% trifluoroacetic acid. The mixture was sonicated for 20 min, then centrifuged, after which the supernatant was removed. This step was repeated, and the combined supernatant was evaporated in a heated water bath under a stream of nitrogen gas for ~60 min until the total sample volume was about 1.5 mL. A total of 6 mL HPLC-grade water was added to each sample, which was sonicated for 0.5 min to dissolve all contents. This mixture was cleaned using solid-phase extraction, eluted with 90% acetonitrile solution, and evaporated to dryness in a heated water bath under a stream of nitrogen. Samples were dissolved in 2 mL HPLC-grade water, sonicated to dissolve all solid contents, and passed through a 0.2-µm syringe filter prior to analysis. Total microcystins were reported as ng toxin · g⁻¹ organic matter.

All data for this study are available at the Auburn University Scholarly Repository, AUrora (<https://aurora.auburn.edu>). Sediment sections analyzed for microcystins were incorporated into a single dataset, and PCA was performed on variables (total microcystins, P, N, organic C, C/N, N/P, aphanizophyll, diatoxanthin, canthaxanthin, beta carotene, and lutein + zeaxanthin) to determine ordination of similar sediment types. PCA was performed using SAS JMP package 7.1. Sediment core Zones (I, II, III, and IV) were determined using *k*-means cluster analysis on the principal components.

Evaluation of Human Effects on Lakes. Because concentrations of cyanobacteria pigments and cyanotoxins are very high in recent sediments (Fig. 2), these variables were replotted on abbreviated scales to highlight stratigraphic fluctuations in these biomarkers during the period of prehistoric Maya occupation (Fig. 3). To place our sediment core in archaeological context, biomarker stratigraphies were compared with periods of Maya prehistory [i.e., the Preclassic, Classic, and Postclassic, established by Coe and Houston (14)] and to highland archaeological phases, defined using pottery styles at Kaminaljuyú (34–36). The dates for the ceramic phases were based on an updated Bayesian dating model (35). Likewise, our core data were compared to previous paleolimnological work (36) and population reconstructions from archaeological findings in the Valley of Guatemala (44). Environmental change in and around Lake Amatitlán was inferred from diatoms, pollen, and nutrient concentrations in a sediment core collected in 2000 at a nearby location (36). Whereas variables associated with nutrient inputs from land use appear to agree between the two cores, indicators of eutrophication [i.e., diatom counts in the Velez et al. (36) record and cyanobacteria pigments in our study] show some discrepancies. Population in the Valley of Guatemala was inferred from archaeological investigation of rural sites, and a chronology was developed using the obsidian dating technique (44). Dates assigned to population changes were corrected from the original publication, using the new chronology of Arroyo et al. (35).

Data Availability. Excel spread sheets data have been deposited in AUrora at the Auburn University Scholarly Repository (<https://aurora.auburn.edu/handle/11200/50011>) (64).

ACKNOWLEDGMENTS. We thank the Autoridad para el Manejo Sustentable de la Cuenca y del Lago de Amatitlán (AMSA) for boat support and lake access. The Universidad del Valle de Guatemala supported the fieldwork and facilitated planning and organization. Alejandra Aguilar and Ninoshka López aided in the fieldwork and core sectioning. We thank Ben Webster for formulating the dating model and making Geographic Information System maps and Avery Lamb for help with cyanotoxin analysis. This work was funded by a National Geographic Society Explorer's Grant (Grant No. HJ-162R-17), an NSF EAGER Grant (Grant No. DEB-1830723), and the Alabama Agricultural Experiment Station.

1. J. Huisman *et al.*, Cyanobacterial blooms. *Nat. Rev. Microbiol.* **16**, 471–483 (2018).
2. Z. E. Taranu *et al.*, Acceleration of cyanobacterial dominance in north temperate-subarctic lakes during the Anthropocene. *Ecol. Lett.* **18**, 375–384 (2015).
3. H. W. Paerl, “Growth and reproductive strategies of freshwater blue-green algae (cyanobacteria)” in *Growth and Reproductive Strategies of Freshwater Phytoplankton*, C. D. Sandgren, Ed. (Cambridge University Press, 1988), pp. 261–315.
4. H. W. Paerl, N. S. Hall, E. S. Calandrino, Controlling harmful cyanobacterial blooms in a world experiencing anthropogenic and climatic-induced change. *Sci. Total Environ.* **409**, 1739–1745 (2011).
5. A. Kaplan *et al.*, The languages spoken in the water body (or the biological role of cyanobacterial toxins). *Front. Microbiol.* **3**, 138 (2012).
6. A. Holland, S. Kinnear, Interpreting the possible ecological role(s) of cyanotoxins: Compounds for competitive advantage and/or physiological aide? *Mar. Drugs* **11**, 2239–2258 (2013).
7. H. W. Paerl, J. Huisman, Climate change: A catalyst for global expansion of harmful cyanobacterial blooms. *Environ. Microbiol. Rep.* **1**, 27–37 (2009).
8. A. M. Dolman *et al.*, Cyanobacteria and cyanotoxins: The influence of nitrogen versus phosphorus. *PLoS One* **7**, e38757 (2012).
9. H. W. Paerl *et al.*, Mitigating a global expansion of toxic cyanobacterial blooms: Confounding effects and challenges posed by climate change. *Mar. Freshw. Res.* **71**, 579–592 (2020).
10. M. A. Burford *et al.*, Perspective: Advancing the research agenda for improving understanding of cyanobacteria in a future of global change. *Harmful Algae* **91**, 101601 (2020).
11. M. L. Wells *et al.*, Future HAB science: Directions and challenges in a changing climate. *Harmful Algae* **91**, 101632 (2020).
12. S. McGowan *et al.*, Ancient blue-green blooms. *Limnol. Oceanogr.* **44**, 436–439 (1999).
13. A. Lami *et al.*, A late glacial and Holocene record of biological and environmental changes form the Crater Lake Albano, Central Italy: An interdisciplinary European project (PALICLAS). *Water Air Soil Pollut.* **99**, 601–613 (1997).
14. M. D. Coe, S. Houston, *The Maya* (Thames & Hudson, ed. 9, 2015).
15. B. W. Leyden, M. Brenner, B. H. Dahlin, Cultural and climatic history of Cobá, a lowland Maya city in Quintana Roo, Mexico. *Quat. Res.* **49**, 111–122 (1998).
16. F. S. Anselmetti, D. A. Hodell, D. Ariztegui, M. Brenner, M. Rosenmeier, Quantification of soil erosion rates related to ancient Maya deforestation. *Geology* **35**, 915–918 (2007).
17. P. M. J. Douglas *et al.*, A long-term decrease in the persistence of soil carbon caused by ancient Maya land use. *Nat. Geosci.* **11**, 645–649 (2018).
18. T. Beach, Soil catenas, tropical deforestation, and ancient and contemporary soil erosion in the Petén Guatemala. *Phys. Geogr.* **19**, 378–405 (1998).
19. D. A. Hodell, J. H. Curtis, M. Brenner, Possible role of climate in the collapse of Classic Maya civilization. *Nature* **375**, 391–394 (1995).
20. D. A. Hodell, M. Brenner, J. H. Curtis, Terminal Classic drought in the northern Maya lowlands inferred from multiple sediment cores in Lake Chichancanab (Mexico). *Quat. Sci. Rev.* **24**, 1413–1427 (2005).
21. M. Medina-Elizalde, E. J. Rohling, Collapse of Classic Maya civilization related to modest reduction in precipitation. *Science* **335**, 956–959 (2012).
22. G. H. Haug *et al.*, Climate and the collapse of Maya civilization. *Science* **299**, 1731–1735 (2003).
23. D. J. Kennett *et al.*, Development and disintegration of Maya political systems in response to climate change. *Science* **338**, 788–791 (2012).
24. P. M. J. Douglas *et al.*, Drought, agricultural adaptation, and sociopolitical collapse in the Maya Lowlands. *Proc. Natl. Acad. Sci. U.S.A.* **112**, 5607–5612 (2015).
25. S. Luzzadder-Beach, T. Beach, Water chemistry constraints and possibilities for ancient and contemporary Maya wetlands. *J. Ethnobiol.* **28**, 211–230 (2008).
26. A. M. Marfia, R. V. Krishnamurthy, E. A. Atekwana, W. F. Panton, Isotopic and geochemical evolution of ground and surface waters in a karst dominated geological setting: A case study from Belize, Central America. *Appl. Geochem.* **19**, 937–946 (2004).
27. S. Luzzadder-Beach, Water resources of the Chunchucmil Maya. *Geograph Rev* **90**, 493–510.
28. D. L. Lentz *et al.*, Molecular genetic and geochemical assays reveal severe contamination of drinking water reservoirs at the ancient Maya city of Tikal. *Sci. Rep.* **10**, 10316 (2020).
29. P. R. Leavitt, D. A. Hodgson, “Sedimentary pigments” in *Tracking Environmental Change Using Lake Sediments, Terrestrial, Algal, and Siliceous Indicators*, J. P. Smol, H. J. P. Birks, W. M. Last, Eds. (Kluwer, Dordrecht, 2001), vol. 3, pp. 295–325.
30. M. N. Waters, C. L. Schelske, M. Brenner, Cyanobacterial dynamics in shallow Lake Apopka (Florida, U.S.A.) before and after the shift from a macrophyte-dominated to a phytoplankton-dominated state. *Freshw. Biol.* **60**, 1571–1580 (2015).
31. A. Zastepa *et al.*, Reconstructing a long-term record of microcystins from the analysis of lake sediments. *Sci. Total Environ.* **579**, 893–901 (2016).
32. M. N. Waters, 4700-year history of cyanobacteria toxin production in a shallow subtropical lake. *Ecosystems (N. Y.)* **19**, 426–436 (2016).
33. A. K. Scherer, Population structure of the Classic period Maya. *Am. J. Phys. Anthropol.* **132**, 367–380 (2007).
34. M. Popenoe de Hatch, E. Ponciano, T. Barrientos Q., M. Brenner, C. Orloff, Climate and technological innovation at Kaminaljuyu, Guatemala. *Anc. Mesoam.* **13**, 103–114 (2002).
35. B. Arroyo *et al.*, Refining Kaminaljuyu chronology: New radiocarbon dates, Bayesian analysis, and ceramic studies. *Lat. Am. Antiq.* **31**, 477–497 (2020).
36. M. I. Velez *et al.*, Environmental and cultural changes in highland Guatemala inferred from Lake Amatitlán sediments. *Geoarchaeology* **26**, 346–364 (2011).
37. L. Pérez *et al.*, Aquatic ecosystems of the Yucatan Peninsula (Mexico), Belize, and Guatemala. *Hydrobiologia* **661**, 407–433 (2011).
38. C. S. Romero-Oliva, V. Contardo-Jara, T. Block, S. Pflugmacher, Accumulation of microcystin congeners in different aquatic plants and crops—A case study from Lake Amatitlán, Guatemala. *Ecotoxicol. Environ. Saf.* **102**, 121–128 (2014).
39. World Health Organization, “Algae and cyanobacteria in fresh water” in *Guidelines for Safe Recreational Water Environments, Vol. 1: Coastal and Fresh Waters* (World Health Organization, Geneva, 2003), pp. 136–158.
40. J. C. Lohse *et al.*, Late Holocene volcanic activity and environmental change in highland Guatemala. *Quat. Sci. Rev.* **191**, 378–392 (2018).
41. M. Blaauw, J. A. Christen, Flexible paleoclimate age-depth models using an autoregressive Gamma process. *Bayesian Anal.* **6**, 457–474 (2013).
42. K. Hesse, E. Dittmann, T. Borner, Consequences of impaired microcystin production for light-dependent growth and pigmentation of *Microcystis aeruginosa* PCC 7806. *FEMS Microbiol. Ecol.* **37**, 39–43 (2001).
43. M. E. L. Estrada, “Estructura, composición y dominancia de las cianobacterias en Lago de Amatitlán, Guatemala y su relación con la pérdida de diversidad de fitoplancton,” Master’s thesis, Universidad de San Carlos de Guatemala (2015).
44. C. N. Murdy, Prehispanic agriculture and its effects in the Valley of Guatemala. *Forest Conser Hist* **34**, 179–190 (1990).
45. W. T. Sanders, C. N. Murdy, “Population and agricultural adaptation in the humid highlands of Guatemala” in *The Historical Demography of Highland Guatemala*, R. M. Carmack, J. Early, C. Lutz, Eds. (Institute of Mesoamerican Studies, Albany, NY, 1982), pp. 23–34.
46. P. R. Leavitt, A review of factors that regulate carotenoids and chlorophyll deposition and fossil pigment abundance. *J. Paleolimnol.* **9**, 109–127 (1993).
47. E. Henao, P. Rzymiski, M. N. Waters, A review of the study of cyanotoxins in paleolimnological research: Current knowledge and future needs. *Toxins (Basel)* **12**, E6 (2019).
48. M. L. Saker, B. A. Neilan, Varied diazotrophies, morphologies, and toxicities of genetically similar isolates of *Cylindrospermopsis raciborskii* (nostocales, cyanophyceae) from Northern Australia. *Appl. Environ. Microbiol.* **67**, 1839–1845 (2001).
49. T. J. Whitmore, M. Brenner, J. H. Curtis, B. H. Dahlin, B. W. Leyden, Holocene climate and human influences on lakes of the Yucatan Peninsula Mexico: An interdisciplinary, palaeolimnological approach. *Holocene* **6**, 273–287 (1996).
50. D. W. Schindler, Eutrophication and recovery in experimental lakes: Implications for lake management. *Science* **184**, 897–899 (1974).
51. C. L. Schelske *et al.*, Abrupt biological response to hydrologic and land-use changes in Lake Apopka, Florida, USA. *Ambio* **34**, 192–198 (2005).
52. M. F. Rosenmeier *et al.*, Recent eutrophication of the southern basin of Lake Peten Itza, Guatemala, human impact on a large tropical lake. *Hydrobiologia* **511**, 161–172 (2004).
53. E. S. Deevey, “Stress, strain, and stability of lacustrine ecosystems” in *Lake Sediments and Environmental History*, E. Y. Haworth, J. W. G. Lund, Eds. (University of Minnesota Press, Minneapolis, 1985), pp. 203–229.
54. M. Tuskada, E. S. Deevey, “Pollen analysis from four lakes in the southern Maya area of Guatemala and El Salvador” in *Quaternary Paleoecology*, E. J. Cushing, H. E. Wright, Eds. (Yale University Press, New Haven, 1967), pp. 303–331.
55. W. T. Sanders, “Chiefdom to state: Political evolution at Kaminaljuyu, Guatemala” in *Reconstructing Complex Societies*, C. Moore, Ed. (The American Schools of Oriental Research, Cambridge, MA, 1974), pp. 97–121.
56. S. F. Borhgeyi, Archaeology in the Maya Highlands. *Sci. Am.* **200**, 100–115 (1959).
57. A. Megged, Nahua patterns of colonization in Maya towns of Guatemala, 1524 to 1582: The indigenous records. *Colonial Lat. Am. Rev.* **22**, 209–234 (2013).
58. E. S. Deevey, Limnological studies in Guatemala and El Salvador. *Int. Assoc. Theoret. Appl. Limnol. Proc.* **12**, 278–283 (1955).
59. M. M. Fisher, M. Brenner, K. R. Reddy, A simple, inexpensive piston corer for collecting undisturbed sediment/water interface profiles. *J. Paleolimnol.* **7**, 157–161 (1992).
60. M. Stuiver, P. J. Reimer, R. W. Reimer, CALIB 8.2 (WWW program) (2021). <http://calib.org/>. Accessed 3 November 2020.
61. D. Harris, W. R. Horwath, C. van Kessel, Acid fumigation of soils to remove carbonates prior to total organic or carbon-13 isotopic analysis. *Soil Sci. Soc. Am. J.* **65**, 1853–1856 (2001).
62. Environmental Protection Agency, Method 6010B: Inductively coupled plasma-atomic emission spectrometry (2014). <https://www.epa.gov/sites/default/files/documents/6010b.pdf>.
63. E. L. Purdie, F. M. Young, D. Menzel, G. A. Codd, A method for acetonitrile-free microcystin analysis and purification by high-performance liquid chromatography, using methanol as mobile phase. *Toxicol. Anal. Chem.* **54**, 887–890 (2009).
64. M. N. Waters *et al.*, Data for: Harmful Algal blooms and cyanotoxins in Lake Amatitlán, Guatemala, coincided with ancient Maya occupation in the watershed. AURora. 10.3509/aurora-81. Deposited 19 October 2021.